Published in final edited form as:
Cancer Res. 2012 April 15; 72(8): 2079–2088. doi:10.1158/0008-5472.CAN-11-3744.

Tumor Vascular Microenvironment Determines Responsiveness to Photodynamic Therapy

Amanda L. Maas[1], **Shirron L. Carter**[1], **E. Paul Wileyto**[2], **Joann Miller**[1], **Min Yuan**[1], **Guoqiang Yu**[3,5], **Amy C. Durham**[4], and **Theresa M. Busch**[1,*]

[1]Department of Radiation Oncology, Perelman School of Medicine, University of Pennsylvania, Philadelphia, PA, USA

[2]Department of Biostatistics and Epidemiology, Perelman School of Medicine, University of Pennsylvania, Philadelphia, PA, USA

[3]Physics and Astronomy, School of Arts and Sciences, University of Pennsylvania, Philadelphia, PA, USA

[4]Department of Pathobiology, School of Veterinary Medicine, University of Pennsylvania, Philadelphia, PA, USA

[5]Center for Biomedical Engineering, University of Kentucky, Lexington, KY

Abstract

The efficacy of photodynamic therapy (PDT) depends upon the delivery of both photosensitizing drug and oxygen. In this study, we hypothesized that local vascular microenvironment is a determinant of tumor response to PDT. Tumor vascularization and its basement membrane (collagen) were studied as a function of supplementation with basement membrane matrix (Matrigel) at the time of tumor cell inoculation. Effects on vascular composition with consequences to tumor hypoxia, photosensitizer uptake and PDT response were measured. Matrigel-supplemented tumors developed more normalized vasculature, composed of smaller and more uniformly-spaced blood vessels than their unsupplemented counterparts, but these changes did not affect tumor oxygenation or PDT-mediated direct cytotoxicity. However, PDT-induced vascular damage increased in Matrigel-supplemented tumors, following an affinity of the photosensitizer Photofrin for collagen-containing vascular basement membrane coupled with increased collagen content in these tumors. The more highly-collagenated tumors demonstrated more vascular congestion and ischemia after PDT, along with a higher probability of curative outcome that was collagen dependent. In the presence of photosensitizer-collagen localization, PDT effects on collagen were evidenced by a decrease in its association with vessels. Together, our findings demonstrate that photosensitizer localization to collagen increases vascular damage and improves treatment efficacy in tumors with greater collagen content. The vascular basement membrane is thus identified to be a determinant of therapeutic outcome in PDT of tumors.

Keywords

collagen; photodynamic therapy; microenvironment; normalization; vasculature

Corresponding Author: Theresa M. Busch, PhD, Department of Radiation Oncology, Perelman School of Medicine, University of Pennsylvania, Anatomy Chemistry Building, Room B13, 3620 Hamilton Walk, Philadelphia, PA 19104-6072, 215-573-3168 (phone), 215-898-0090 (fax), buschtm@mail.med.upenn.edu.

Conflicts of interest: none

Introduction

Tumor microenvironment is a variable to be contended with in the delivery of chemotherapy, radiation, and photodynamic therapy, among other therapeutic modalities (1, 2). Tumor vascularization is especially important in photodynamic therapy (PDT), which relies on blood vessels to deliver the molecular oxygen and photosensitizing drugs that are required for a successful outcome to typically applied protocols. Yet, a chaotic vascular network in many tumors limits drug and oxygen delivery (3–5). Heterogeneities in both photosensitizer levels and oxygen concentrations have been documented within and between tumors in preclinical and clinical studies (6–10). Moreover, use of approaches to adjust for these heterogeneities has met with success in improving treatment outcome (11–13).

Several investigations demonstrate effects of tumor microenvironment on PDT. Chen et al (14) studied rat prostate tumors grown in orthotopic vs. subcutaneous sites, showing that tumors grown in the prostate exhibited a higher vascular density and lower hypoxic fractions than those in subcutaneous tissue. This improvement in oxygenation was accompanied by greater PDT-mediated cytotoxicity in the prostate-localized tumors. Others showed the rate of photosensitizer diffusion through tumors of the same cell line to differ as a function of the anatomical site of their propagation, suggesting a role for tumor microenvironment in photosensitizer uptake and distribution (15). The significance of the tumor stroma in PDT was considered in a review by Peng and Nesland (16), who noted an affinity of photosensitizers for collagen, which could lead to differences in photosensitizer uptake among tumors as a function of their stromal composition.

Herein this report, we sought to identify specific features of the tumor vasculature responsible for mediating a PDT effect, hypothesizing that the local vascular microenvironment is a determinant of PDT response. Toward this goal, tumor cells were co-inoculated in mouse hosts with Matrigel Basement Membrane Matrix (17) to create an altered tumor microenvironment that included changes to the vasculature. The effects of vascular microenvironment on tumor oxygenation, photosensitizer concentrations and localization, and PDT-created vascular damage were measured. From these studies, we have identified an *in vivo* role for collagen IV, a component of the tumor basement membrane, in determining the response of tumor vasculature to PDT.

Materials and Methods

Tumor Models

H460 cells were purchased from ATCC, while RIF and SCCVII cells originated from the lines produced by Twentyman et al (18) and O'Malley et al (19), respectively. All cells were authenticated by Radil (Columbia, MO) in January, 2012 by PCR. RIF, SCCVII or H460 tumors were propagated by intradermal injection of $3x10^5$ (RIF) or $1x10^6$ (SCVVII and H460) cells in C3H (RIF and SCCVII) or nude (H460) mice (NCI-Frederick, Frederick, MD). Matrigel-supplemented tumors had Matrigel Basement Membrane Matrix (4.5 mg/ml; BD Bioscience, San Jose, CA) added to the tumor cell suspension. Animals were studied ~7–10 days later when tumors were 5–7 mm in diameter. Fur in C3H mice was clipped and the treatment area depilated at least 24h before illumination.

Immunohistochemistry

Tumor blood vessels and basement membrane were identified by staining of frozen sections (14μm) with antibodies to CD31 (BD Pharmingen, San Diego, CA) and collagen (Millipore Corporation, Temecula, CA), respectively. After ethanol fixation sections were stained for collagen (1:40 for 1h) and CD31 (1:100 for 1h) as previously described (20), with the exception that rabbit serum replaced milk and bovine serum albumin in collagen staining.

Respective to the collagen and CD31 antibodies, secondary antibodies of FITC-conjugated rabbit anti-goat (1:200 for 1h; Jackson Immunoresearch, West Grove, PA) and Cy5-conjugated mouse anti-rat (1:50 for 45 min; Jackson Immunoresearch) were used. Hoechst 33342 (20 μM) was used to label tissue. Images (10x) were collected by a Nikon Eclipse 800 fluorescence microscope and Photometrics Quantix CCD digital camera controlled by IPLab software (see Supplementary Material), then masked to label stained areas and analyzed for % of Hoechst-identified tumor positive for CD31 or collagen. Additionally, CD31-stained vessels were identified as unique "objects" based on contiguous staining, from which intervascular spacing, vascular density, and vessel size were measured. Analyses utilized routines in the MATLAB Image toolbox (MathWorks, Natick MA), except for collagen and Hoechst masking (created in Adobe Photoshop; Adobe Systems Inc, San Jose, CA). Controls included slides stained with only secondary antibody, and demonstrated no staining.

Hypoxia labeling

Tumor hypoxia was identified via flow cytometry (FACSCalibur) after EF3 [(2-(2-nitroimidazol-1[H]-yl)-N-(3,3,3-trifluoropropyl)acetamide) labeling. EF3 (52 mg/kg) was administered in two inoculations to increase tumor concentrations (i.v. followed 1h later by i.p). At 2h after i.p. EF3 delivery, tumors were excised, enzymatically digested, and stained (Cy5-conjugated ELK5-A8 antibody (21)). Mean Cy5 fluorescence was read in the FL4 channel (λ_{ex}=635nm, λ_{em}=661nm). Nonspecific antibody binding was measured after incubation of antibody in the presence of 1.0 mM EF3.

Photodynamic therapy

Animals received Photofrin (available from Pinnacle Biologics, Bannockburn, IL) i.v. and microlens-tipped fibers (Pioneer, Bloomfield, CT) were used to deliver 632±3 nm light from a Ceralas diode laser (Biolitec AG, Jena, Germany). Laser output was measured with a LabMaster power meter (Coherent, Auburn, CA) and adjusted to deliver 75 mW/cm^2 at the tumor surface. Mice were anesthetized by inhalation of isoflurane in medical air (VetEquip anesthesia machine, Pleasanton, CA). Animal studies were approved by the University of Pennsylvania Institutional Animal Use and Care Committee; animal facilities are AAALAC accredited.

In vivo/in vitro clonogenic assay

Excised tumors were weighed, minced, and enzymatically digested over 30 min (37°C) as previously described (22). The number of clonogenic cells per g was calculated as the number of cells per g times the ratio of the number of colonies counted to the number plated.

Photosensitizer distribution and concentration

Fluorescence microscopy (see Supplementary Material) for Photofrin was performed immediately after sectioning. Sections were then stained (see *Immunohistochemistry)* and re-photographed at the same coordinates. From masks of CD31, collagen and Photofrin, vascular "objects" with Photofrin colocalization were analyzed for their % coverage by Photofrin (MATLAB). The extent of Photofrin colocalization was compared between "objects" consisting of CD31-stained vasculature and those consisting of collagenated vasculature identified by both CD31 and collagen staining.

Tumor concentrations of Photofrin were quantified using spectrofluorometric assay (23), as we have previously described (8).

Diffuse correlation spectroscopy

Tumor relative blood flow during PDT was measured using diffuse correlation spectroscopy (DCS) (24). This technology measures rapid temporal fluctuations of transmitted light (785nm) through tissues and uses the auto-correlation functions associated with these fluctuations to extract information about the motion of tissue scatterers, in this case red blood cells. Data were collected as a function of the separation distance between the source and detector pairs in the optical probe, averaged, and then normalized to flow values (in the same tumor) in the two minutes before PDT began.

Histopathology

Tumors were excised at 3h after PDT, fixed, embedded, sectioned and stained with Masson's trichrome (Pathology Core Laboratory, Children's Hospital of Philadelphia) or H&E (Ryan Veterinary Hospital, University of Pennsylvania). The extent of vascular congestion was quantified as the pixel count of congestion, relative to the tumor-containing area on the section.

Tumor response

Mice were followed after PDT until tumor volumes >400 mm^3 (RIF and SCCVII) or pre-treatment volume (H460). Volume was measured in two orthogonal directions (volume = diameter x $width^2$ x 3.14/6). A cure was defined as an absence of tumor regrowth at 90 days after PDT.

Confocal microscopy

Frozen sections (20 μm) collected immediately after PDT were stained for CD31 and collagen (see *Immunohistochemistry*) and imaged (10X) on a Zeiss LSM 510 Confocal Microscope controlled by AIM confocal software (see Supplementary Material). Colocalization analysis (in Volocity 5; Perkin Elmer; Waltham, Massachusetts) utilized the overlap coefficient, k, which reported on the contribution of collagen signal intensity to "objects" identified as blood vessels based on collagen/CD31 colocalization.

Statistical analysis

Differences in immunohistochemical or histological staining between naïve and Matrigel-supplemented tumors were compared using t-tests assuming unequal variance, as were differences in photosensitizer content and tumor blood flow. Paired t-tests were used to compare the extent of Photofrin colocalization with CD31-labeled blood vessels vs. the collagen-containing areas on these vessels. Analyses were performed in JMP (SAS Institute, Inc; Cary, NC) with $p < 0.05$ considered significant.

Results

Matrigel-altered tumor microenvironment doesn't change PDT-mediated direct tumor cytotoxicity

Tumors with an altered vascular microenvironment were grown without changing the malignant cell type or anatomic location of propagation by supplementing the cell inoculum with Matrigel. Compared to unsupplemented (naïve) RIF tumors, Matrigel-supplemented tumors were more consistently vascularized (note the avascular strip in the RIF tumor of Fig 1A). Overall, RIF-Matrigel tumors contained significantly *less* vascular area (Fig 1B), which could be attributed to a small decrease in vessel size (not shown) and a significant reduction in the vascular density (Fig 1C). These changes are consistent with vascular normalization (25).

Following observations of more consistent vascularization in RIF-Matrigel tumors, intervascular distance (median) was measured in RIF (42μm) and RIF-Matrigel tumors (44μm), but found to be indistinguishable between the tumor types (Fig 1D). In contrast, variability in intervascular spacing was much larger in RIF tumors, and, accordingly, the coefficient of variation was significantly ($p = 0.016$) higher in these tumors (28 ± 3% vs. 10 ± 3% in RIF-Matrigel tumors, Fig 1E). To determine how these changes in vascularization may affect oxygenation, hypoxia was labeled by EF3. Both models exhibited more EF3 binding (mean ± SE) than nonspecific background (3.57 ± 0.34), but no differences were found between RIF-Matrigel (29 ± 8) and RIF tumors (32 ± 6). Any improvement in tumor oxygenation could increase direct PDT cytotoxicity (11) so the *in vivo/in vitro* clonogenic assay was used to measure cell death immediately after treatment (5 mg/kg Photofrin, 24 h, 75 mW/cm^2, 135 J/cm^2). Mean (± SE) clonogenic survivals were 2.12 ± 0.9e7 and 1.47 ± 0.5e7 clonogenic cells/g in RIF and RIF-Matrigel tumors, respectively. Thus, in addition to the EF3 data, the absence of a differential in direct PDT-mediated cytotoxicity suggests that changes in the vascular status of RIF-Matrigel tumors didn't improve their oxygenation.

Photosensitizer localization is affected by microenvironment

Vascular normalization can affect uptake or retention of therapeutic drugs (26), leading us to next assess Photofrin distributions at the gross and microscopic levels. Gross accumulation of Photofrin was visible in both RIF and RIF-Matrigel tumors, but drug pooling among heterogeneously-distributed vasculature was evident in RIF tumors (composites in Fig 2, grayscale original in Fig S1). Given this substantial pooling, it was not surprising that RIF tumors had a significantly higher ($p = 0.003$) bulk photosensitizer uptake (median ± SE) of 4.5 ± 0.6 ng/mg, compared to 1.4 ± 0.2 ng/mg in RIF-Matrigel tumors (inset, Fig 2).

At the microscopic level, Photofrin associated with vasculature, localizing to ~15–30% of the area occupied by a blood vessel when averaged across the vessels in each tumor section. Moreover, the vascular localization of Photofrin increased when analysis was restricted to vessel areas that contained collagen IV, a component of vascular basement membrane (Fig 3A). By paired analysis, Photofrin associated significantly ($p<0.001$) better with collagen-containing areas of blood vessels compared to the entire vessel. Because collagen is a major component of Matrigel, the collagen composition of RIF and RIF-Matrigel tumors was compared. Collagen was more prominent in RIF-Matrigel tumors (Fig 3B) with an average (±SE) content of 9.3 ± 1.2% in RIF-Matrigel tumors vs. 4.9 ± 0.5% in RIF tumors ($p=0.007$) (Fig 3C).

Vascular response to PDT is enhanced in a more highly-collagenated tumor microenvironment

The preferred association of photosensitizer with collagenated areas on blood vessels (in Fig 3A), together with the increased collagen content of Matrigel-supplemented RIF tumors (in Fig 3C) led us to suspect that the Matrigel-altered microenvironment would have increased susceptibility to PDT-mediated vascular damage. To test if vascular response differed as a function of microenvironment, DCS was used to follow tumor hemodynamics during PDT. After an acute increase, blood flow decreased during PDT (Fig 4A), in agreement with our previous report (24). No difference in the pattern or magnitude of change in blood flow during PDT was noted between the groups, for example, mean (± SE) relative blood flow in the last two minutes of PDT was 0.72 (± 0.10) in RIF vs. 0.63 (± 0.08) in RIF-Matrigel tumors ($p=0.48$). However, greater intratumor variability in vascular response was detectable in RIF tumors, which is plotted as error bars in the representative examples. The average (± SE) coefficient of variation in blood flow during PDT was 14.0 ± 2.6% vs. 6.9 ± 0.9% in RIF vs. RIF-Matrigel tumors, respectively, which documents a significant decrease ($p= 0.02$) in the intratumoral heterogeneity of vascular response in RIF-Matrigel tumors.

A more homogeneous vascular response in the more highly-collagenated RIF-Matrigel tumors could be mediated through collagen's role as a substrate in the coagulation cascade (27). PDT can activate this cascade, causing vascular congestion and fibrin accumulation *in vivo* (28, 29). In both naïve and Matrigel-supplemented tumors, PDT-created vascular congestion with accompanying fibrin accumulation was detectable by H&E (Supplementary Fig. S2). RIF-Matrigel tumors had a significantly larger ($p=0.029$) congested area (mean ± SE) of 10.5 ± 1.0% (vs. 6.2 ± 0.9% in RIF tumors; Fig 4B,C), and significantly ($p=0.03$) greater ischemia after treatment (Fig 4D).

Tumor response studies confirmed the therapeutic significance of the stronger vascular response in RIF-Matrigel tumors (Fig 4E). Whereas all RIF tumors regrew within 24 days, 25% of RIF-Matrigel tumors didn't recur (tumor cures). It is noteworthy that PDT was less effective in RIF tumors despite their higher photosensitizer levels. This is consistent with the observed ineffective distribution of photosensitizer to avascular areas (see Fig 2). Conversely, lower gross levels of photosensitizer in RIF-Matrigel tumors weren't prohibitive of a robust vascular and curative tumor response, pointing to the significance of photosensitizer localization to these results.

Better outcome in more highly-collagenated tumors requires extravascular photosensitizer localization

Augmentation of vascular and tumor damage in more highly-collagenated tumors occurred in the context of Photofrin association with vascular collagen. To evaluate if collagen content affected response when photosensitizer localization to collagen didn't occur, Photofrin-PDT (2.5 mg/kg) was performed with a short drug-light interval. No tumor or stromal localization of Photofrin was detectable after 30 minutes (Fig 5A), in contrast to results with standard (24h) incubation (Fig 5A, inset). PDT of RIF tumors to 75 J/cm^2 with a short drug-light interval produced a regrowth delay of up to 21 days, similar to that reported above for standard PDT. However, unlike that found with standard PDT, RIF-Matrigel tumors weren't more responsive than RIF tumors when drug-light interval was short. A curative light dose (135 J/cm^2) at short drug-light interval also failed to differentially affect response in RIF vs. RIF-Matrigel tumors (Fig 5B). Thus, the extravascular distribution of Photofrin, including to basement membrane, is necessary for tumors to differentially benefit from PDT when they are more-highly collagenated. It points to a role for PDT effect on collagen in mediating increases in vascular damage in Matrigel-supplemented tumors.

The absence of a differential response between RIF and RIF-Matrigel tumors to PDT with short drug-light interval also provides evidence that Matrigel doesn't impart therapeutic advantage to PDT independent of vascular response. To independently confirm this finding, we studied H460 tumors, which unlike RIF, demonstrate high collagen content in their naïve form (12.8 ± 1.7%). The strength and distribution of collagen staining in H460 tumors (Supplementary Fig. S3A), reflects that seen in RIF-Matrigel tumors (see Fig 1A), and no measureable increase in collagen accompanied the addition of Matrigel to H460 tumors (13.7 ± 0.7%). H460 tumors had an 18% cure rate to Photofrin-PDT and the addition of Matrigel didn't improve response, further confirming that Matrigel itself didn't inherently benefit PDT (Fig S3B).

PDT alters collagen expression

Having defined a role for Photofrin localization to collagen as a determinant of tumor response in RIF tumors, SCCVII tumors were evaluated in confirmatory studies that investigated PDT effect on collagen. SCVVII-Matrigel tumors demonstrated collagen levels similar to RIF-Matrigel tumors, i.e. 9.0 ± 1.5% vs. 9.3 ± 1.2%, respectively, which was, on average, more collagen then the 6.7 ± 0.7% found in naïve SCVVII tumors (Fig 6A). As

expected, Photofrin was significantly ($p = 0.003$) better associated with collagenated areas of blood vessels than with the entire structure (Fig 6B). Moreover, as found in the RIF models, SCCVII-Matrigel tumors were more responsive to PDT than their naïve counterparts (Fig 6C), with a cure rate of 57% in the Matrigel-supplemented vs. 0% in naïve tumors, respectively.

Given the high response rate of SCCVII-Matrigel tumors, this model was employed for further investigation of PDT effect on vessel structure. Using confocal microscopy, vessels were identified as areas of collagen and CD31 colocalization. A representative micrograph (Fig 6D) illustrates a control tumor with CD31-labeled blood vessels (red) that were well-covered by collagen (green). Contrastingly, in tumors that received PDT, areas of vasculature that lack collagen coverage were more prominent. The inset of Fig 6D plots the overlap coefficient (k), which quantifies the contribution of signal from one channel (i.e. collagen) to its colocalization with another channel (i.e. collagen and CD31). The change in collagen visualization upon PDT could be attributed to a decrease in the contribution of collagen to the vessel signal, indicating that PDT leads to alterations in vascular collagen.

Discussion

Herein this manuscript we establish a role for tumor collagen composition as a determinant of PDT therapeutic effect. The data show that photosensitizer localization to collagen-containing vascular basement membrane augments PDT response of tumors with greater collagen content. Increases in vascular congestion, decreases in tumor perfusion, and evidence of collagen disruption after PDT all suggest that vascular damage leads to improvements in curative outcome in more highly-collagenated tumors. This conclusion is further supported by findings that photosensitizer localization to collagen is necessary for more highly-collagenated tumors to experience a therapeutic advantage. Collagen is a major structural component of vascular basement membrane, and is prominent, but variable, in its association with tumor vasculature (30). Thereby these results have important implications in the clinical setting wherein significant heterogeneity in tumor microenvironment, including its blood vessels, can exist (31, 32).

In the anatomy of a blood vessel, basement membrane provides structural support abluminal to endothelial cells and separates these cells from underlying stroma (33). Damage to endothelial cells can expose basement membrane, triggering the coagulation cascade through complexes of platelets and vonWillebrand factor that bind to exposed collagen (27). Tumors are commonly characterized by inconsistencies in the endothelial cell layer, which can make them more prone to such damage (26). The chain of vascular events during PDT has been proposed to include endothelial cell rounding, basement membrane exposure and subsequent occlusive platelet aggregation (28). Our results are consistent with these mechanisms, as shown by the development of vascular congestion and reductions in tumor perfusion. However, we additionally document that *1)* these effects are significantly stronger (more vascular congestion, greater reductions in perfusion) in tumors with greater collagen content and *2)* photosensitizer localization to collagen is necessary for more highly-collagenated tumors to exhibit a differential tumor response. This begets the obvious question of how collagen may play a role in vascular response to PDT.

An answer to this question initiates from our observation that collagen is a target of photosensitizer localization within a blood vessel. This finding is in agreement with *in vivo* observation of Photofrin fluorescence in collagen-containing areas (34) and *in vitro* demonstration of photosensitizer binding to collagen (35, 36). Furthermore, our *in vivo* data demonstrate an effect of PDT on collagen. Confocal imaging documented a decrease in collagen association with blood vessels in PDT-treated tumors. This decrease is detected by

reductions in antibody staining of collagen, which could result from damage to the binding site or its masking by PDT-induced structural alterations (37) or fibrin accumulation (28). Yet, irrespective of which mechanism dominated, this change in collagen staining establishes an effect of PDT on collagen that is consistent with the “bleaching” of collagen expression found in thrombotic veins (38) and thus connects our observations of collagen photosensitization with those of vascular congestion and fibrin accumulation. *In vitro* studies by Fungaloi et al (39) further support a role for collagen photosensitization in augmenting vascular damage. They report that PDT of a collagen matrix promotes the adhesion of platelets to this matrix. When occurring *in vivo*, such platelet adhesion would be part of the coagulation cascade that leads to vascular congestion and ischemia, both of which increased in more highly-collagenated tumors and accordingly bore out the implications of Fungaloi’s report.

In addition to differences in collagen composition, other microenvironmental distinctions were apparent between naïve and Matrigel-supplemented tumors. Matrigel supplementation served to support vascular development (17), facilitating the growth of tumors with a lower density of smaller, more uniformly-spaced blood vessels. Thus, these data also serve to describe the mechanisms by which Matrigel can stimulate tumor development in xenograft hosts. That said, in the present study, tumor take was already 100% without supplementation, so any vascular change introduced by Matrigel provided no advantage in this regard. A normalized vasculature structure could potentially improve drug or oxygen concentrations, but we found no benefit to either. In agreement, others have also reported that vascular normalization failed to improve tumor oxygenation. Tailor et al (40) published that papzopanib produced vascular changes consistent with normalization in human tumor xenografts, such as decreased vascular density, yet this was accompanied by increased hypoxia. Similarly, Riesterer et al (41) reported that antiangiogenic treatment directed toward vascular normalization reduced vascular densities, but increased hypoxia in mammary carcinoma tumors. The broad range of tumor volumes, from 175–425 mm^3, included in this study suggests that a failure of vascular normalization to improve tumor oxygenation can occur independent of tumor size.

We employed Matrigel for altering microenvironment because it offers the advantages that it didn’t involve a change in tumor histologic type, alter the anatomical location of tumor propagation (e.g. in subcutaneous vs. orthotopic tumors) or require identification of a timeframe of vascular restructuring (e.g. when antiangiogenics are used). Even more importantly, increases in collagen content in Matrigel-supplemented tumors were biologically relevant. Collagen accounted for 9.0 ± 1.5% and 9.3 ± 1.2% of the tumor in SCCVII-Matrigel and RIF-Matrigel tumors, respectively. Contrastingly, H460 tumors (without Matrigel) were composed of 12.8 ± 1.7% collagen. Accordingly, the extent of collagen staining in the Matrigel-supplemented tumors is similar to that which occurs in another unaltered tumor model, and we can conclude that Matrigel supplementation, under the conditions employed, didn’t lead to unrealistically high collagen expression.

Abnormal collagen deposition in vascular basement membrane is common in tumors (26, 42) and inconsistencies in its association with endothelial cells lead to clinical observations that range from losses in (43) to thickening of (44) basement membrane. Studies of vascular basement membrane in human tumors illustrate that the limited extent of collagen positivity in our preclinical models are relevant to that seen clinically. For example, tumors from 27 of 32 patients with rectal cancer demonstrated little to no staining for collagen expression (45). Similarly, in glioblastomas and pilocytic astrocytomas, collagen content was ~3% (range ~1–8%) of the tumor area (46). Encouragingly, data from the present study suggest that just small increases in collagen composition (e.g. to ~10%) can serve to augment PDT response. It therefore may be possible to use pharmaceutical approaches to increase tumor collagen

content prior to PDT. For example, an antibody to VEGF-receptor increased vascular basement membrane in a murine mammary carcinoma at three days after its administration, in concert with decreases in vascular density and vascular diameter (4). Other approaches to increase collagen could include local injection of collagen-based tissue fillers, as used in plastic surgery (47), or subcurative ionizing radiation (48) .

Modulation of tumor microenvironment prior to delivery of radiation or chemotherapeutics has a demonstrated benefit in preclinical (49, 50) and potential in clinical studies (26). The present study has investigated how PDT may be affected by tumor vascular microenvironment. Our findings provide the first evidence that tumor collagen composition is an important microenvironmental variable in vascular and therapeutic response of tumors to PDT. They serve to identify vascular basement membrane as a therapeutically-relevant target for pretreatment alteration in tumors to receive PDT.

Supplementary Material

Refer to Web version on PubMed Central for supplementary material.

Acknowledgments

We are grateful to Elizabeth Rickter, Andrea Stout and Kevin Jenkins for assistance with animals, confocal, and MATLAB, respectively, as well as to Prof Arjun Yodh for advice on DCS.

Grant Support

This work was supported by NIH CA-087971, CA-085831, and CA-129554.

Financial support: This work was supported by the NIH (CA-087971, CA-085831 and CA-129554).

References

1. Maity A, Bernhard EJ. Modulating tumor vasculature through signaling inhibition to improve cytotoxic therapy. Cancer Res. 2010; 70:2141–5. [PubMed: 20179191]
2. Casas A, Di Venosa G, Hasan T, Al B. Mechanisms of resistance to photodynamic therapy. Curr Med Chem. 2011; 18:2486–515. [PubMed: 21568910]
3. Matsumoto S, Batra S, Saito K, Yasui H, Choudhuri R, Gadisetti C, et al. Antiangiogenic agent sunitinib transiently increases tumor oxygenation and suppresses cycling hypoxia. Cancer Res. 2011; 71:6350–9. [PubMed: 21878530]
4. Tong RT, Boucher Y, Kozin SV, Winkler F, Hicklin DJ, Jain RK. Vascular normalization by vascular endothelial growth factor receptor 2 blockade induces a pressure gradient across the vasculature and improves drug penetration in tumors. Cancer Res. 2004; 64:3731–6. [PubMed: 15172975]
5. Vlahovic G, Ponce AM, Rabbani Z, Salahuddin FK, Zgonjanin L, Spasojevic I, et al. Treatment with imatinib improves drug delivery and efficacy in NSCLC xenografts. Br J Cancer. 2007; 97:735–40. [PubMed: 17712313]
6. Busch TM, Hahn SM, Wileyto EP, Koch CJ, Fraker DL, Zhang P, et al. Hypoxia and Photofrin uptake in the intraperitoneal carcinomatosis and sarcomatosis of photodynamic therapy patients. Clin Cancer Res. 2004; 10:4630–8. [PubMed: 15269134]
7. Zhou X, Chen B, Hoopes PJ, Hasan T, Pogue BW. Tumor vascular area correlates with photosensitizer uptake: analysis of verteporfin microvascular delivery in the Dunning rat prostate tumor. Photochem Photobiol. 2006; 82:1348–57. [PubMed: 17421078]
8. Hahn SM, Putt ME, Metz J, Shin DB, Rickter E, Menon C, et al. Photofrin uptake in the tumor and normal tissues of patients receiving intraperitoneal photodynamic therapy. Clin Cancer Res. 2006; 12:5464–70. [PubMed: 17000681]

9. Igbaseimokumo U. Quantification of in vivo Photofrin uptake by human pituitary adenoma tissue. J Neurosurg. 2004; 101:272–7. [PubMed: 15309918]
10. Stylli SS, Howes M, MacGregor L, Rajendra P, Kaye AH. Photodynamic therapy of brain tumours: evaluation of porphyrin uptake versus clinical outcome. J Clin Neurosci. 2004; 11:584–96. [PubMed: 15261226]
11. Huang Z, Chen Q, Shakil A, Chen H, Beckers J, Shapiro H, et al. Hyperoxygenation enhances the tumor cell killing of photofrin-mediated photodynamic therapy. Photochem Photobiol. 2003; 78:496–502. [PubMed: 14653582]
12. Zhou X, Pogue BW, Chen B, Demidenko E, Joshi R, Hoopes J, et al. Pretreatment photosensitizer dosimetry reduces variation in tumor response. Int J Radiat Oncol Biol Phys. 2006; 64:1211–20. [PubMed: 16504761]
13. Busch TM, Xing X, Yu G, Yodh A, Wileyto EP, Wang HW, et al. Fluence rate-dependent intratumor heterogeneity in physiologic and cytotoxic responses to Photofrin photodynamic therapy. Photochem Photobiol Sci. 2009; 8:1683–93. [PubMed: 20024165]
14. Chen B, Pogue BW, Zhou X, O'Hara JA, Solban N, Demidenko E, et al. Effect of tumor host microenvironment on photodynamic therapy in a rat prostate tumor model. Clin Cancer Res. 2005; 11:720–7. [PubMed: 15701861]
15. Zhou X, Pogue BW, Chen B, Hasan T. Analysis of effective molecular diffusion rates for verteporfin in subcutaneous versus orthotopic Dunning prostate tumors. Photochem Photobiol. 2004; 79:323–31. [PubMed: 15137508]
16. Peng Q, Nesland JM. Effects of photodynamic therapy on tumor stroma. Ultrastruct Pathol. 2004; 28:333–40. [PubMed: 15764581]
17. Kleinman HK, Martin GR. Matrigel: basement membrane matrix with biological activity. Semin Cancer Biol. 2005; 15:378–86. [PubMed: 15975825]
18. Twentyman PR, Brown JM, Gray JW, Franko AJ, Scoles MA, Kallman RF. A new mouse tumor model system (RIF-1) for comparison of end-point studies. J Natl Cancer Inst. 1980; 64:595–604. [PubMed: 6928244]
19. O'Malley BW Jr, Cope KA, Johnson CS, Schwartz MR. A new immunocompetent murine model for oral cancer. Arch Otolaryngol Head Neck Surg. 1997; 123:20–4. [PubMed: 9006499]
20. Busch TM, Wileyto EP, Emanuele MJ, Del Piero F, Marconato L, Glatstein E, et al. Photodynamic therapy creates fluence rate-dependent gradients in the intratumoral spatial distribution of oxygen. Cancer Res. 2002; 62:7273–9. [PubMed: 12499269]
21. Busch TM, Hahn SM, Evans SM, Koch CJ. Depletion of tumor oxygenation during photodynamic therapy: detection by the hypoxia marker EF3 [2-(2-nitroimidazol- 1[*H*]-yl)-*N*-(3,3,3,-trifluoropropyl)acetamide]. Cancer Res. 2000; 60:2636–42. [PubMed: 10825135]
22. Busch TM, Wang HW, Wileyto EP, Yu G, Bunte RM. Increasing damage to tumor blood vessels during motexafin lutetium-PDT through use of low fluence rate. Radiat Res. 2010; 174:331–40. [PubMed: 20726728]
23. Bellnier DA, Greco WR, Parsons JC, Oseroff AR, Kuebler A, Dougherty TJ. An assay for the quantitation of Photofrin in tissues and fluids. Photochem Photobiol. 1997; 66:237–44. [PubMed: 9277143]
24. Yu G, Durduran T, Zhou C, Wang HW, Putt ME, Saunders HM, et al. Noninvasive monitoring of murine tumor blood flow during and after photodynamic therapy provides early assessment of therapeutic efficacy. Clin Cancer Res. 2005; 11:3543–52. [PubMed: 15867258]
25. Escorcia FE, Henke E, McDevitt MR, Villa CH, Smith-Jones P, Blasberg RG, et al. Selective killing of tumor neovasculature paradoxically improves chemotherapy delivery to tumors. Cancer Res. 2010; 70:9277–86. [PubMed: 21045141]
26. Goel S, Duda DG, Xu L, Munn LL, Boucher Y, Fukumura D, et al. Normalization of the vasculature for treatment of cancer and other diseases. Physiol Rev. 2011; 91:1071–121. [PubMed: 21742796]
27. Chen J, Lopez JA. Interactions of platelets with subendothelium and endothelium. Microcirculation. 2005; 12:235–46. [PubMed: 15814433]

28. Fingar VH, Wieman TJ, Haydon PS. The effects of thrombocytopenia on vessel stasis and macromolecular leakage after photodynamic therapy using photofrin. Photochem Photobiol. 1997; 66:513–7. [PubMed: 9337624]
29. Dolmans DE, Kadambi A, Hill JS, Waters CA, Robinson BC, Walker JP, et al. Vascular accumulation of a novel photosensitizer, MV6401, causes selective thrombosis in tumor vessels after photodynamic therapy. Cancer Res. 2002; 62:2151–6. [PubMed: 11929837]
30. Baluk P, Morikawa S, Haskell A, Mancuso M, McDonald DM. Abnormalities of basement membrane on blood vessels and endothelial sprouts in tumors. Am J Pathol. 2003; 163:1801–15. [PubMed: 14578181]
31. Nagy JA, Chang SH, Dvorak AM, Dvorak HF. Why are tumour blood vessels abnormal and why is it important to know? Br J Cancer. 2009; 100:865–9. [PubMed: 19240721]
32. Carmeliet P, Jain RK. Principles and mechanisms of vessel normalization for cancer and other angiogenic diseases. Nat Rev Drug Discov. 2011; 10:417–27. [PubMed: 21629292]
33. LeBleu VS, Macdonald B, Kalluri R. Structure and function of basement membranes. Exp Biol Med (Maywood). 2007; 232:1121–9. [PubMed: 17895520]
34. Peng Q, Nesland JM, Moan J, Evensen JF, Kongshaug M, Rimington C. Localization of fluorescent Photofrin II and aluminum phthalocyanine tetrasulfonate in transplanted human malignant tumor LOX and normal tissues of nude mice using highly light-sensitive video intensification microscopy. Int J Cancer. 1990; 45:972–9. [PubMed: 2139867]
35. Musser DA, Wagner JM, Datta-Gupta M. The interaction of tumor localizing porphyrins with collagen and elastin. Res Commun Chem Pathol Pharmacol. 1982; 36:251–9. [PubMed: 7100629]
36. el-Far MA, Pimstone NR. The interaction of tumour-localizing porphyrins with collagen, elastin, gelatin, fibrin and fibrinogen. Cell Biochem Funct. 1985; 3:115–9. [PubMed: 3836016]
37. Pazos MC, Nader HB. Effect of photodynamic therapy on the extracellular matrix and associated components. Braz J Med Biol Res. 2007; 40:1025–35. [PubMed: 17665038]
38. Vosko MR, Rother J, Friedl B, Bultemeier G, Kloss CU, Hamann GF. Microvascular damage following experimental sinus-vein thrombosis in rats. Acta Neuropathol. 2003; 106:501–5. [PubMed: 12904994]
39. Fungaloi P, Statius van Eps R, Wu YP, Blankensteijn J, de Groot P, van Urk H, et al. Platelet adhesion to photodynamic therapy-treated extracellular matrix proteins. Photochem Photobiol. 2002; 75:412–7. [PubMed: 12003132]
40. Tailor TD, Hanna G, Yarmolenko PS, Dreher MR, Betof AS, Nixon AB, et al. Effect of pazopanib on tumor microenvironment and liposome delivery. Mol Cancer Ther. 2010; 9:1798–808. [PubMed: 20515941]
41. Riesterer O, Honer M, Jochum W, Oehler C, Ametamey S, Pruschy M. Ionizing radiation antagonizes tumor hypoxia induced by antiangiogenic treatment. Clin Cancer Res. 2006; 12:3518–24. [PubMed: 16740778]
42. Baluk P, Hashizume H, McDonald DM. Cellular abnormalities of blood vessels as targets in cancer. Curr Opin Genet Dev. 2005; 15:102–11. [PubMed: 15661540]
43. Liu SY, Chang LC, Pan LF, Hung YJ, Lee CH, Shieh YS. Clinicopathologic significance of tumor cell-lined vessel and microenvironment in oral squamous cell carcinoma. Oral Oncol. 2008; 44:277–85. [PubMed: 17475541]
44. Winkler F, Kozin SV, Tong RT, Chae SS, Booth MF, Garkavtsev I, et al. Kinetics of vascular normalization by VEGFR2 blockade governs brain tumor response to radiation: role of oxygenation, angiopoietin-1, and matrix metalloproteinases. Cancer Cell. 2004; 6:553–63. [PubMed: 15607960]
45. Jayne DG, Heath RM, Dewhurst O, Scott N, Guillou PJ. Extracellular matrix proteins and chemoradiotherapy: alpha5beta1 integrin as a predictive marker in rectal cancer. Eur J Surg Oncol. 2002; 28:30–6. [PubMed: 11869010]
46. Sie M, de Bont ES, Scherpen FJ, Hoving EW, den Dunnen WF. Tumour vasculature and angiogenic profile of paediatric pilocytic astrocytoma; is it much different from glioblastoma? Neuropathol Appl Neurobiol. 2010; 36:636–47. [PubMed: 20704656]
47. Eppley BL, Dadvand B. Injectable soft-tissue fillers: clinical overview. Plast Reconstr Surg. 2006; 118:98e–106e.

48. Kozin SV, Winkler F, Garkavtsev I, Hicklin DJ, Jain RK, Boucher Y. Human tumor xenografts recurring after radiotherapy are more sensitive to anti-vascular endothelial growth factor receptor-2 treatment than treatment-naive tumors. Cancer Res. 2007; 67:5076–82. [PubMed: 17545583]

49. Cerniglia GJ, Pore N, Tsai JH, Schultz S, Mick R, Choe R, et al. Epidermal growth factor receptor inhibition modulates the microenvironment by vascular normalization to improve chemotherapy and radiotherapy efficacy. PLoS One. 2009; 4:e6539. [PubMed: 19657384]

50. McGee MC, Hamner JB, Williams RF, Rosati SF, Sims TL, Ng CY, et al. Improved intratumoral oxygenation through vascular normalization increases glioma sensitivity to ionizing radiation. Int J Radiat Oncol Biol Phys. 2010; 76:1537–45. [PubMed: 20338480]

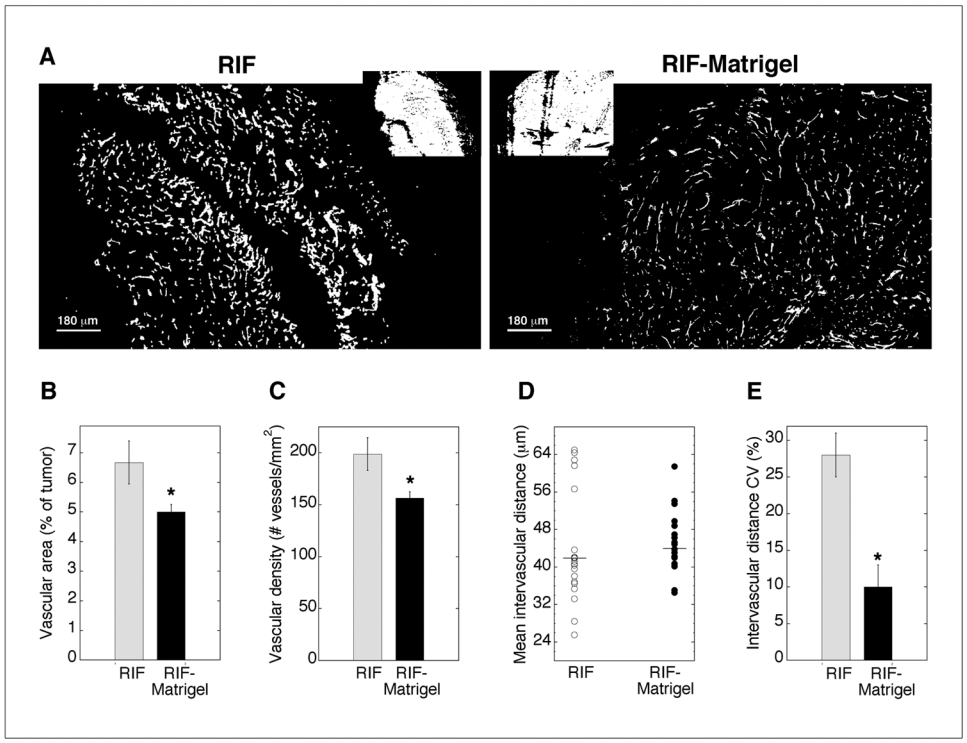

Fig 1.

Vascularization of RIF vs. RIF-Matrigel tumors. Representative masked images of CD31-identified vasculature (A; insets of Hoechst staining). Mean (±SE) vascular area (B) and vascular density (C) for 21–22 sections (3 depths from 4–5 tumors). On individual sections, mean intervascular distance was calculated (D; horizontal line indicates median), and the coefficient of variation (E) measured to assess intratumor heterogeneity in vascular spacing (n=4–5 animals). *indicates $p<0.05$ for differences between RIF and RIF-Matrigel tumors.

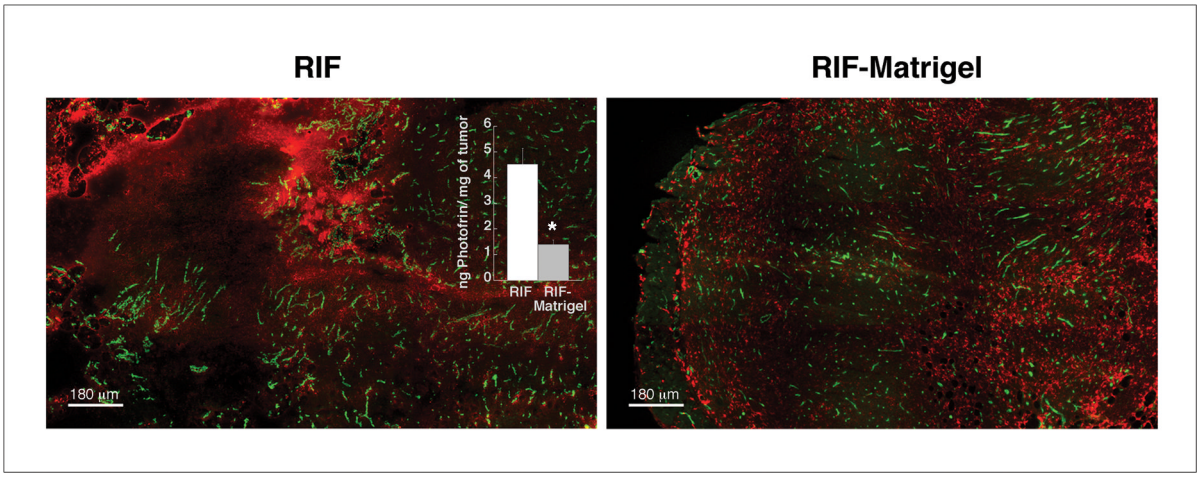

Fig 2.

Photofrin distribution and uptake in RIF vs. RIF-Matrigel tumors. Merged and pseudocolored images of Photofrin (red) and blood vessels (green) after 24h of *in vivo* (5 mg/kg) exposure. Intensity levels are adjusted for optimal viewing of drug distribution, not for comparison of drugs levels. Drug levels (median ± SE) are quantified in the inset by spectrofluorometric analysis (n=4–6 mice). *indicates $p<0.05$ for differences between RIF and RIF-Matrigel tumors.

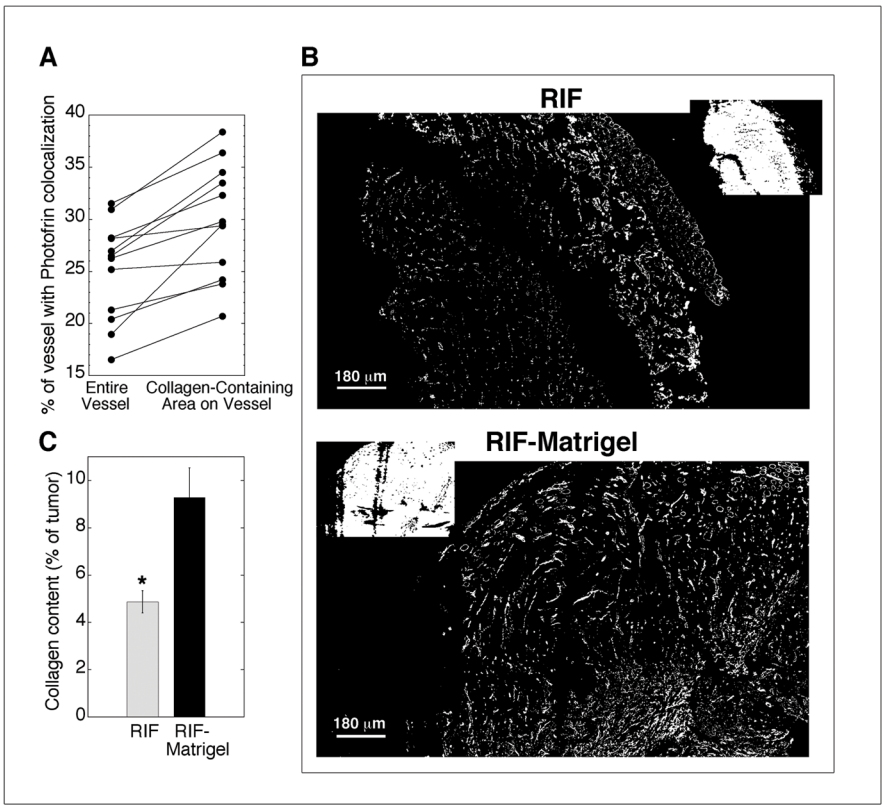

Fig 3.

Photofrin association with tumor vasculature and its basement membrane in RIF vs. RIF-Matrigel tumors. Mean % area that Photofrin colocalizes with “objects” identified as vessels or collagenated vessels (A) in 12 sections (from 3 depths and 2 tumors). Representative masked images of collagen (B; insets of Hoechst staining with corresponding CD31 staining in Fig 1A) and mean area (± SE) of collagen expression (C) for 21–22 sections (3 depths from 4–5 tumors). *indicates $p<0.05$ for differences between RIF and RIF-Matrigel tumors.

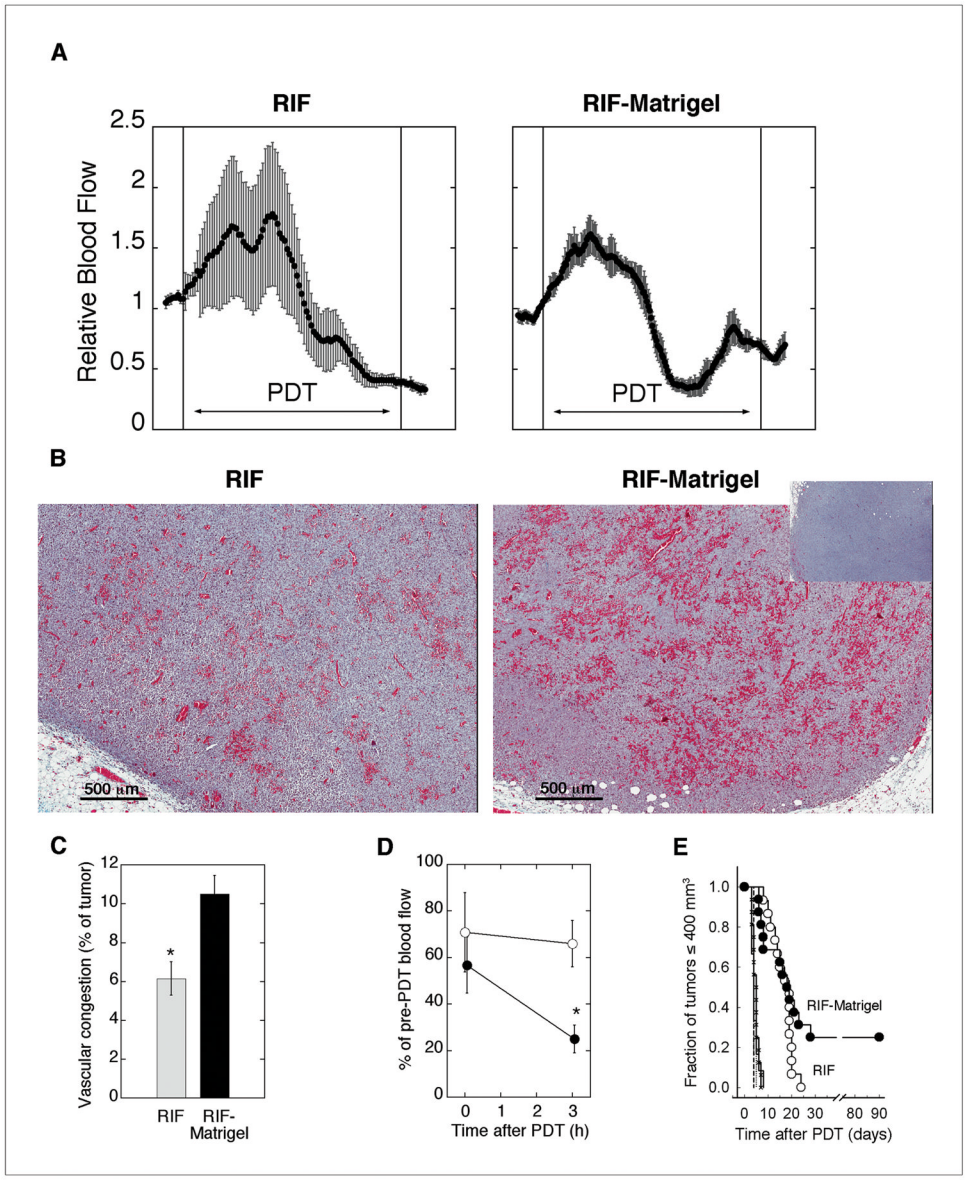

Fig 4.

Vascular response to PDT. Representative traces of relative tumor blood flow during PDT, with error bars indicating intratumor heterogeneity (A). Vascular congestion (3h post-PDT) in representative images of Mason-Trichrome stained sections (B; inset of untreated tumor) and mean (±SE) tumor area of vascular congestion (C; n=3 tumors). Post-PDT decreases in blood flow (mean ± SE) for RIF (open circles, n=3) and RIF-Matrigel (closed circles, n=4) tumors (D) and Kaplan-Meier plots (E) of long-term tumor response (n=15–16 in treated groups). Controls include untreated RIF (dashed line, n=5), untreated RIF-Matrigel (dotted line, n=6), light-only (solid line, n=12), and Photofrin-only (crosshatch, n=16). PDT with Photofrin (5 mg/kg, 24h), 135 J/cm^2, 75 mW/cm^2. *indicates $p<0.05$ for differences between RIF and RIF-Matrigel tumors.

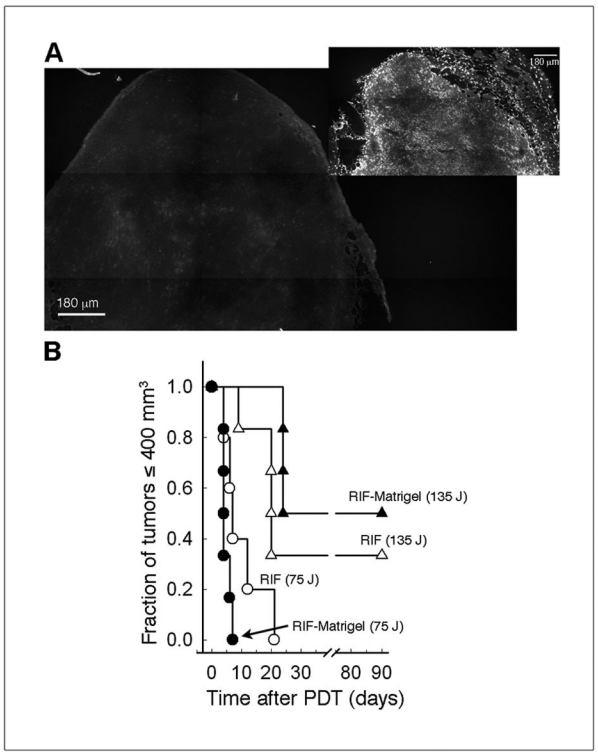

Fig 5.

Photosensitizer distribution and tumor response to PDT with short drug-light interval. Representative images of Photofrin distribution in RIF-Matrigel tumors after *in vivo* exposure to 2.5 mg/kg for 30 min (A) or 5 mg/kg for 24h (inset); note that blood-localized photosensitizer isn't retained during sample processing and thus isn't visible in these images. Long-term PDT response (B) in RIF (open symbols, n=5) and RIF-Matrigel (closed symbols, n=6) tumors treated with 75 (circles) or 135 (triangles) J/cm^2 (75 mW/cm^2) at 30 minutes after Photofrin (2.5 mg/kg) administration.

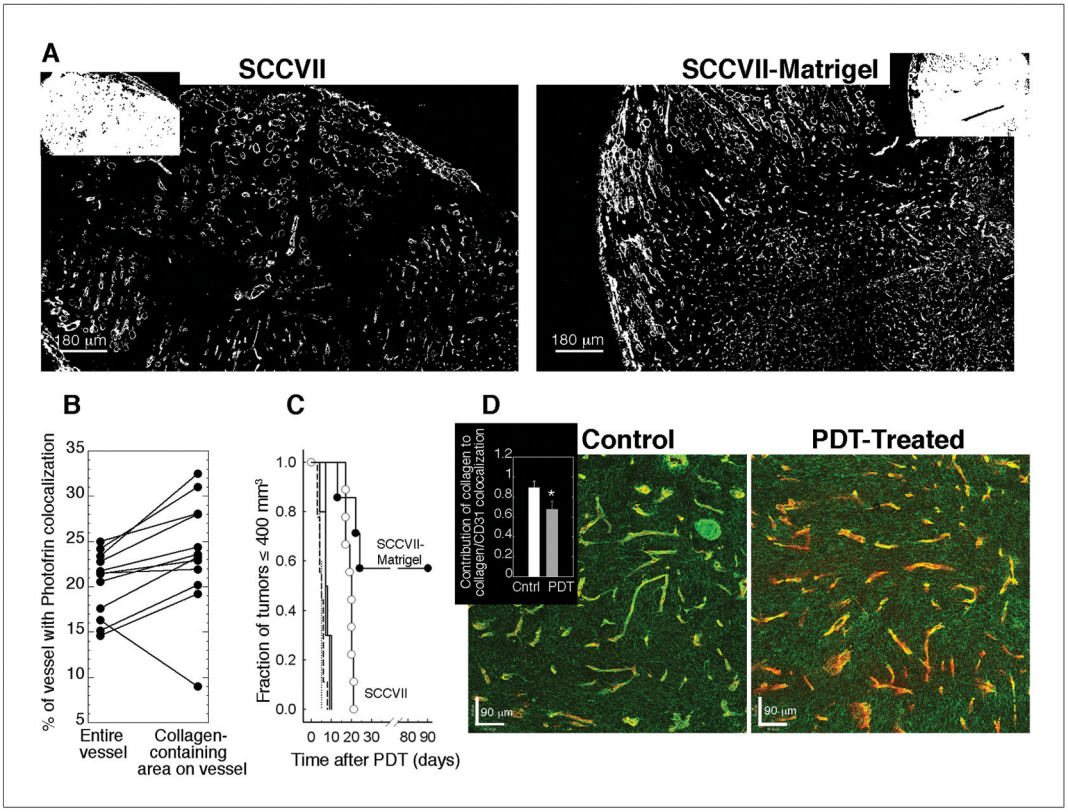

Fig 6.

Tumor microenvironment and PDT response in naïve vs. Matrigel-supplemented SCCVII tumors. Representative masked images of collagen (A; insets of Hoechst staining). Mean % area that Photofrin colocalizes with “objects” identified as vessels or collagenated vessels (B) in 15 sections (from 2–3 depths and 6 tumors). Long-term PDT response (C) in SCCVII (open circles, n=9) and SCVVII-Matrigel (closed circles, n=7) tumors; controls indicate untreated SCVVII (dashed line, n=9), untreated SCCVII-Matrigel (dotted line, n=5), light-only (solid line, n=10), and Photofrin-only (crosshatch, n=10). From confocal microscopy (D) the individual contributions of collagen (green) and CD31 (red) to their colocalization is shown for untreated (left) and PDT-treated (right) SCCVII-Matrigel tumors; inset summarizes the overlap coefficient for collagen contribution to vascular staining (mean ± SE; n=5). PDT with Photofrin (5 mg/kg, 24h), 135 J/cm^2, 75 mW/cm^2. *indicates $p<0.05$ for a decrease with PDT.